Since January 2020 Elsevier has created a COVID-19 resource centre with free information in English and Mandarin on the novel coronavirus COVID-19. The COVID-19 resource centre is hosted on Elsevier Connect, the company's public news and information website.

Virology 510 (2017) 273–280

Contents lists available at ScienceDirect

Virology

journal homepage: www.elsevier.com/locate/yviro

Human bocavirus 1 infection of CACO-2 cell line cultures

Lucía María Ghietto, Ana Paola Toigo D'Angelo, Franco Agustin Viale, María Pilar Adamo*

Instituto de Virología "Dr. J. M. Vanella", Facultad de Ciencias Médicas, Universidad Nacional de Córdoba, Argentina

ARTICLE INFO

Keywords:
Primate bocaparvovirus 1
Isolation
Virus replication
Sequence

ABSTRACT

Human bocavirus 1 (HBoV1) is a parvovirus associated with pneumonia in infants. It has been detected in different tissues, including colorectal tumors. In this study, we investigated whether Caco-2 cell line, derived from human colon cancer, can be utilized as a model for HBoV1 replication. We demonstrate HBoV1 replication in Caco-2 cultures supplemented with DEAE-dextran after inoculation with respiratory material from infected patients presenting with acute respiratory infection. A viral cycle of rapid development is displayed. However, in spite of HBoV1 DNA 4-fold increment in the supernatants and monolayers by day 1, evidencing that the system allows the virus genome replication after the entry occurred, infectious progeny particles were not produced. These results are consistent with an infection that is limited to a single growth cycle, which can be associated to mutations in the NS1 and VP1/VP2 regions of HBoV1 genome. Further research will contribute to fully elucidate these observations.

1. Introduction

Human bocavirus 1 (HBoV1) belongs to the species *Primate bocaparvovirus 1* in the genus *Bocaparvovirus*, subfamily *Parvovirinae*, family *Parvoviridae* (Qiu et al., 2017). It causes lower acute respiratory tract infections (ARTI) especially in infants less than 2 years old (Ghietto et al., 2015; Martin et al., 2009; Meriluoto et al., 2012), and the frequency of detection varies from 1% to 33% (Bicer et al., 2013; Garcia-Garcia et al., 2008; Ghietto et al., 2012b; Martin et al., 2009). Severe cases are associated with high viral load, anti-HBoV1 IgM antibody detection or an increase in the levels of IgG antibodies, comorbidity and age (Christensen et al., 2010; Ghietto et al., 2015; Nascimento-Carvalho et al., 2012; Wang et al., 2010). A longitudinal study of children from infancy to puberty documented a clear association of primary HBoV1 infection with respiratory symptoms (Meriluoto et al., 2012). All of that strongly supports the etiological role of HBoV1 in ARTI.

In vitro, HBoV1 viral particles from nasopharyngeal clinical specimens infect polarized primary human airway epithelium cultures developed at an air-liquid interface (HAE-ALI) (Dijkman et al., 2009). Other authors obtained HBoV1 virions from HEK293 cells transfected with an infectious plasmid and demonstrated that this reverse genetic system generated HBoV1 virions that productively infect HAE-ALI at a high multiplicity of infection (MOI) -using 750 viral genome copies per cell- and cause cytopathic effect (Deng et al., 2014, 2013; Huang et al., 2012; Khalfaoui et al., 2016). On the other hand, HBoV1 DNA was detected in tissue from tonsils, adenoids (Gunel et al., 2015; Norja et al., 2012), lung and colorectal tumors (Abdel-Moneim et al., 2016; Schildgen et al., 2013), providing evidence of the capacity of the virus to infect different cell types.

In this study, we investigated whether epithelial cells derived from human colorectal adenocarcinoma (Caco-2) can be utilized as a model for HBoV1 replication. We demonstrate HBoV1 replication in Caco-2 cell culture supplemented with diethylaminoethyl-dextran (DEAE-dextran) after inoculation with respiratory material from HBoV1-infected patients with ARTI.

2. Materials and method

2.1. Inoculum preparation

The inoculum was prepared from HBoV1-positive respiratory secretions obtained by nasopharyngeal aspirate from two children. Samples 2526 and 307 had different virus concentrations 1.34×10^9 DNA copies/μl and 1.14×10^3 DNA copies/μl, respectively. These two samples were used for high- and low-MOI assays. The patients from whom the clinical specimens were obtained were 9 and 10 years old and were hospitalized due to lower respiratory tract illness. They were hemoculture negative and also negative by molecular method (real time RT-PCR) for other common respiratory viruses, such as influenza A and B, parainfluenza 1, -2 and -3, adenovirus, respiratory syncytial virus and metapneumovirus (Ghietto et al., 2015). HBoV1 was

* Correspondence to: Instituto de Virología "Dr. J. M. Vanella", Facultad de Ciencias Médicas, UNC, Calle Enf. Gordillo Gómez S/N, Ciudad Universitaria, CP 5016 Córdoba, Argentina.
E-mail address: mpadamo@fcm.unc.edu.ar (M.P. Adamo).

http://dx.doi.org/10.1016/j.virol.2017.07.034
Received 30 May 2017; Received in revised form 27 July 2017; Accepted 28 July 2017
Available online 01 August 2017
0042-6822/

confirmed by sequencing [Gen' database accession numbers JX034732 and JN632491 (Ghietto et al., 2012b, 2015)]. Fifty-µl respiratory secretion was diluted in 500 µl Eagle's Minimum Essential Medium (EMEM) (GIBCO) with penicillin-streptomycin, centrifuged 3 min at 1000*g* and filtered. This preparation was re-tested by PCR and qPCR, aliquoted and kept at − 70 °C until used in the infection assays.

2.2. Cell cultures

Human colon adenocarcinoma Caco-2 cells (ATCC® HTB-37), and Vero cells (ATCC ® CCL-81) were grown in EMEM (GIBCO) supplemented with penicillin-streptomycin or gentamicin, glutamine and 10% fetal bovine serum (FBS); this is referred to as complete growth medium. Cell monolayers were trypsinized and reseeded every 6 or 7 days, using 0.25% trypsin and 0.02% EDTA, and maintained at 37 °C in a 5% CO_2 incubator. To obtain differentiated Caco-2 cultures, the cells were placed in 6-well plates with 3 ml complete growth medium. After the cells reached 100% confluence, the cultures were maintained during 4 weeks with changes of the supernatant medium every 5–7 days until use. In these cultures, after reaching confluence the cells differentiate spontaneously under normal culture conditions into enterocyte-like cells, developing tight junctions and expressing transporters found in the small intestine. These cells are homogeneously polarized and differentiated after 30 days (Buhrke et al., 2011; Lnenickova et al., 2016).

2.3. Experimental conditions and HBoV1 infection

Control (mock–infected) and infected Caco-2 and Vero cultures were maintained in EMEM culture medium, standard or supplemented with 1 or 10 µg/ml of DEAE-dextran. DEAE-dextran is a polycationic derivative of the carbohydrate polymer dextran. It was one of the first chemical reagents used to transfer nucleic acids into cultured mammalian cells (Vaheri and Pagano, 1965) and has been used to enhance the growth of other viruses such as coronaviruses, rubella, and picornaviruses. Postinoculation temperatures of incubation were 33 °C or 37 °C. Previous studies described that respiratory viruses replicated slightly better at 33 °C than at 37 °C, since the lower temperature seems to replicate the conditions in the upper respiratory tract (Gangl et al., 2015; Papadopoulos et al., 1999). Three independent repetitions of infection assays were performed in 60 mm-Petri dishes. During the optimization of DEAE-dextran concentration to be used in the culture, we observed cytotoxicity and decreased cell survival in the control and infected cultures supplemented with 10 µg/ml DEAE-dextran. Consequently, the assays with DEAE-dextran were performed at 1 µg/ml.

Cultures were washed with phosphate-buffered saline (PBS) and 50-µl virus suspension prepared as indicated before was directly inoculated on the cells. At the moment of inoculation, regular cultures were 70–80% confluent monolayers and differentiated cultures were multilayers of 30 days. The virus was allowed to adsorb for 1 h at 37 °C or 33 °C. Next, the inoculum was removed and fresh culture medium was added (standard or supplemented with DEAE-dextran). Samples from the supernatant medium and the cells attached to the substratum were collected at 0 h postinfection (hpi) to 6 days postinfection (dpi). The samples at time point “0 hpi” corresponded to medium or cells collected immediately after inoculation (that is, following the addition of 50 µl-inoculum, removing it and adding fresh culture medium). Sterile EMEM or DEAE-dextran EMEM were used in as controls of reagents. Additionally, a negative nasopharyngeal aspirate (for HBoV1 and all the other above mentioned common respiratory viruses), obtained from a 1 year old patient hospitalized with lower ARTI, was processed exactly as the HBoV1+ specimen and inoculated into cultures to serve as negative control of infection.

Blind passage assays (8 successive passages after the starting culture inoculated with the diluted and filtered clinical specimens) were performed with inoculums from both samples 307 and 2526. For the blind passage assays, a 50-µl aliquot of supernatant or monolayers taken at 48 hpi from these cultures was used to infect fresh cultures. This procedure was repeated six more times. To release the intracellular virions, monolayers were lysed by 3 freeze-thaw cycles. Control cultures as explained above were also included in the series. Samples from the supernatant medium and the cell monolayer were preserved for virus detection in every passage.

Infected monolayers of Caco-2 cells were subcultured using the standard technique for cell passage, in order to determine if a persistent infection could be established. Sequences of 5 passages were performed, with a 1:5 dilution rate of the cell suspension at each passage. In addition, Caco-2 cell cultures were infected at 70–80% confluence and maintained during 28 dpi with changes of supernatant media every 5–7 days.

2.4. Nucleic acid extraction and HBoV1 detection

Nucleic acids were extracted from 200 µl of supernatant and 20 cm^2 monolayers using Axyprep Body Fluid Viral DNA/RNA Miniprep Kit (Axygen Bioscience). Extracts were stored at − 20 °C for subsequent HBoV1 detection. HBoV1 was detected by PCR as described previously (Ghietto et al., 2012a). PCR products were visualized in 8.5% polyacrylamide gels stained with silver solution (0.11 M $AgNO_3$).

2.5. Determination of cytopathic effect in cell culture

Cultures were observed daily under a reversed phase light microscopy to determinate cytopathic effect (CPE). To monitor the morphological changes in the monolayers photographs were taken at intervals of 24 h until 6 dpi. Sample monolayers were fixed with cold methanol and stained with hematoxylin-eosin.

2.6. HBoV1 quantification

HBoV1 DNA load in the supernatant and monolayers 1–6 dpi from Caco-2 and Vero cultures maintained in the different conditions described was determined by absolute quantification in Applied Biosystems 7500 Real-Time PCR System equipment, using the NP1 gene as the target (Allander et al., 2007). Samples of supernatant medium and cells attached to the surface form Caco-2 cultures at 3, 6 and 12 hpi were also quantified. The viral load value of the samples at 0 hpi were interpreted as remnants of the inoculum. The PCR protocol was essentially as described elsewhere (Ghietto et al., 2015), with 25 µl of amplification reaction final volume containing 2.5 µl of DNA sample, 5 U/µl of Platinum Taq DNA polymerase (Invitrogen), 0.04 µM each primer and 0.1 µl of a 1/100 SYBR Green (Invitrogen S-7563) dilution in DMSO. The viral load in each sample was calculated from a standard curve performed with a synthetic oligonucleotide (Marcrogen Korea) of known concentration.

2.7. Immunofluorescence assay

In order to confirm the infection of Caco-2 cells, an immunofluorescence assay (IFA) was optimized using as primary antibody a pool of sera obtained from children in whom HBoV1 respiratory infection had been confirmed. During the procedure, different concentrations of first antibody, conjugate antibody, and blocking solution as well as incubation time and washings were tested. The definite IFA applied was as follows: the cultures were fixed at 24 and 96 hpi, using freshly prepared 4% paraformaldehyde, for 20 min at room temperature. Cells were then permeabilized with 1% NP40, 5 min at room temperature and blocked with 5% bovine serum albumin, 1 h at 37 °C. The primary antibody was added at a 1/1000 dilution in 5% bovine serum albumin, incubating overnight at 4 °C. Subsequently, the conjugate antibody (FITC-anti-human IgG) was added at a 1/400 dilution and incubated

for 1 h at 37 °C. Each step was preceded by three washes with PBS, 5 min each. To corroborate the immunofluorescence pattern, a volume of pooled HBoV1+ sera at a 1/500 dilution was preincubated during 1 h at 37 °C with an equal volume of supernatant or cell lysate (obtained after 3 freeze-thaw cycles), for a 1/1000 final dilution of the primary antibody. These depleted pooled sera were then used in immunofluorescence assays as described above. Two controls of infection were included: sterile medium and negative nasopharyngeal aspirate.

The slides were prepared with FluorSave (EMD Millipore) and observed under epifluorescence microscope IX81 Olympus Motorized Inverted Research. Imaging Software: Cell M.

2.8. Genome sequence analysis

DNA extracted from the supernatant medium and the cells in the monolayer at 6 dpi were used for sequence analysis. We aimed to amplify the complete genome of HBoV1 by PCR with 5 µl of DNA sample in a total volume of 50 µl per reaction. This included 0.25 mM dNTP mix, 5 U of Platinum Taq DNA polymerase (Invitrogen) per µl and the primers described previously (Cardozo Tomas et al., 2015) at a concentration of 0.40 µM. PCR products were visualized in 2% agarose gels stained with GelRed™ (Biotum) and purified using a QIAGEN PCR cleanup kit. Sequencing reactions were performed bidirectionally using appropriate primers and cycle-sequencing kits (ABI PRISM BigDye Terminator v. 3.1; PE Applied Biosystems), and resolved in a 3700 Genetic Analyzer (Applied Biosystems). Sequence analysis was performed using the Molecular Evolutionary Genetics Analysis (MEGA 6) software.

2.9. Statistical analysis

Viral load values in different culture condition were compared using analysis of variance (ANOVA) test with a level of significance $p < 0.05$. Three independent replications of quantitative infection assays were performed and averages and standard deviations were calculated.

Accession numbers: KY629421, KY629422 and KY629423

3. Results

3.1. HBoV infection of Caco-2 and Vero cultures

The PCR tests with Caco-2 and Vero cultures inoculated with clinical material from HBoV1-infected patients and maintained in the different conditions described rendered the results shown in Table 1. HBoV1 was detected in 100% of the Caco-2 cell cultures during all the incubation time that the experiment lasted, either at 33 °C or at 37 °C, when the culture medium was supplemented with DEAE-dextran, but never in the controls. In the absence of DEAE the virus detection was less conspicuous. In contrast, in Vero cells culture no positive monolayers were observed under the same conditions (Table 1). Inoculated cultures did not show CPE (changes in cell morphology) or cell survival, as compared with the controls (sterile medium and processed negative clinical specimen). Representative pictures are shown in Fig. 1.

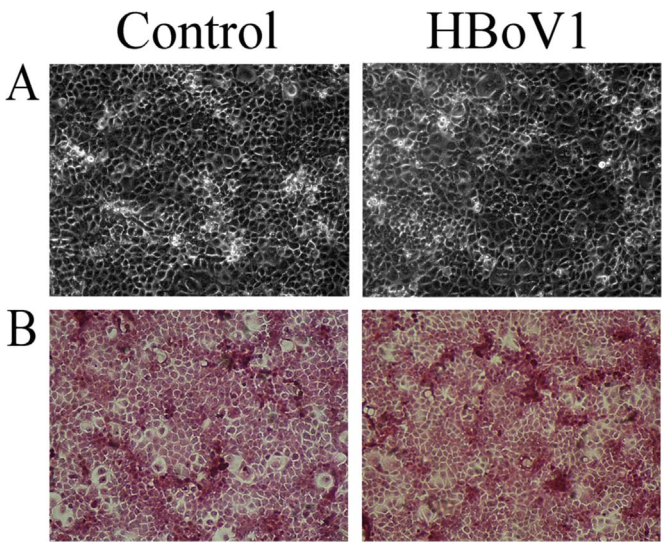

Fig. 1. Micrograph of Caco-2 cells infected with HBoV1 at 37 °C, 6 dpi. A. in vivo monolayer EMEM-DEAE-dextran. B. Fixed and stained with hematoxylin-eosin monolayer EMEM-DEAE-dextran. 20X.

Differentiated Caco-2 cultures inoculated with EMEM-DEAE-dextran 1 µg/ml were also positive at 24 and 48 hpi viral DNA was detected in the monolayers but not in the supernatant medium (data not shown). Again, microscopy showed no CPE or any apparent changes in cell survival (Fig. 2).

3.2. Quantification of HBoV1 in Caco-2 and Vero cell culture

The two clinical specimens used to prepare the inoculum had different concentrations: sample 307 had 1.34×10^9 DNA copies/µl while sample 2526 had 1.14×10^3 DNA copies/µl. However, comparable evolution of the virus titer was observed in cultures inoculated with both virus preparations in Caco-2 cell cultures maintained at 37 °C supplemented with DEAE-dextran. Viral DNA concentration increased 3–4-fold in the supernatants and monolayers by day 1. After that, the viral load remained constant in the supernatants but fluctuated in the monolayers (Fig. 3A). Cultures at 33 °C initially showed a comparable progression; then, towards day 6 pi, the virus titer in supernatant fell (Fig. 3B). Given the results of virus detection by qualitative PCR (Table 1), only samples from the supernatant medium of Vero cell cultures were quantified. As shown in Fig. 4C, the viral load in these cultures decreased during the first 4 days of infection, and then the virus reached titers that were 4-fold less compared to those in Caco-

Table 1
HBoV1 PCR detection in monolayers and supernatants 1–6 dpi in Caco-2 and Vero cell culture in different conditions. S: supernatant. M: monolayer.

Culture conditions			1 dpi		2 dpi		3 dpi		4 dpi		5 dpi		6 dpi	
			S	M	S	M	S	M	S	M	S	M	S	M
Caco-2	Standard EMEM	37 °C	+	-	+	-	+	-	+	+	+	+	+	-
		33 °C	-	-	+	-	-	-	-	-	+	-	-	-
	DEAE-dextran-EMEM	37 °C	+	+	+	+	+	+	+	+	+	+	+	+
		33 °C	+	+	+	+	+	+	+	+	+	+	+	+
Vero	Standard EMEM	37 °C	-	-	+	-	+	-	+	-	+	-	+	-
		33 °C	+	-	-	-	-	-	+	-	-	-	+	-
	DEAE-dextran-EMEM	37 °C	+	-	+	-	+	-	-	-	-	-	+	-
		33 °C	+	-	-	-	-	-	+	-	-	-	+	-

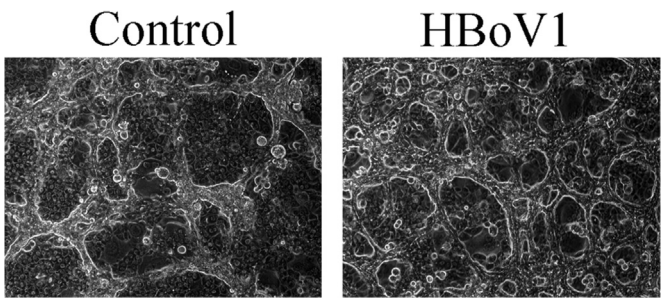

Fig. 2. Micrograph of in vivo differentiated Caco-2 cultures infected with HBoV1 in the presence of DEAE-dextran at 37 °C, 6 dpi. 20X.

2 cells. Viral titers in Caco-2 and Vero cultures at day 6 pi were statistically different (p = 0.0004).

A 4-fold increase in the viral load was also observed in differentiated Caco-2 cell multilayers by 48 hpi, not significantly different (p > 0.05) form Caco-2 monolayers (Fig. 4).

3.3. Immunofluorescence assay to HBoV1 in Caco-2 cell cultures

A unique pattern was observed in Caco-2 monolayers inoculated with HBoV1 in the presence of DEAE-dextran. At 24 and 96 hpi fluorescent foci of a spotted arrangement were detected, mainly located in the perinuclear region of the cells. This pattern, as portrayed in the representative images of Fig. 5, was consistently detected in infected cultures (albeit in scatter foci) but never observed in the control cultures (sterile medium and negative sample).

To corroborate the previous results we carried out an antibody depletion assay, where the antibodies present in the pool of human sera were allowed to react with virus particles in the medium supernatant and cell lysate form infected Caco-2 monolayers (HBoV1 was detected in these cultures by PCR), followed by immunofluorescence test. As shown in Fig. 6, when the pooled sera had been pretreated with infected supernatants and cell lysates (and depleted of specific antibodies), the former fluorescence pattern of infected cultures was not observed.

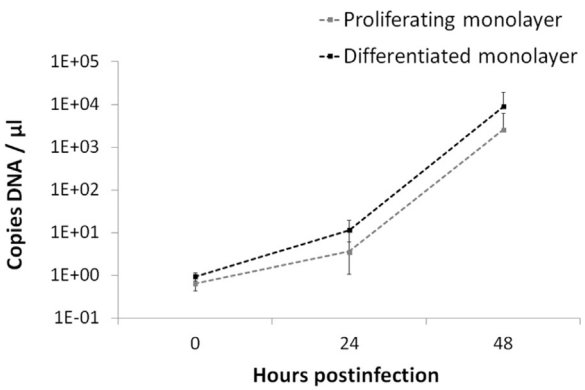

Fig. 4. HBoV1 DNA concentration (copies of DNA/µl) in proliferating and differentiated Caco-2 monolayer culture at 37 °C EMEM-DEAE-dextran at different hours postinfection (x axis) inoculated with sample 2526.

In the blind passage series, no blind passage tested positive by PCR; only the supernatants and monolayers from the starting cultures were positive (with both inoculums). Similarly, assays to determine if a chronic infection could be established rendered detection of HBoV1 only in supernatant and monolayer of the initial infected culture; samples of subcultured infected Caco-2 cell monolayers were negative by PCR. On the other hand, infected Caco-2 cultures maintained at 37 °C with DEAE-EMEM produced viruses that could be demonstrated in the attached cells for as long as 4 weeks (80 copies DNA/µl at 28 dpi), without any detectable CPE.

3.4. HBoV1 sequence analysis

The virus detected in the supernatant and monolayer at 6 dpi was subjected to sequence analysis. To sequence the complete genome, we targeted 8 consecutive and overlapping fragments. Respect to the

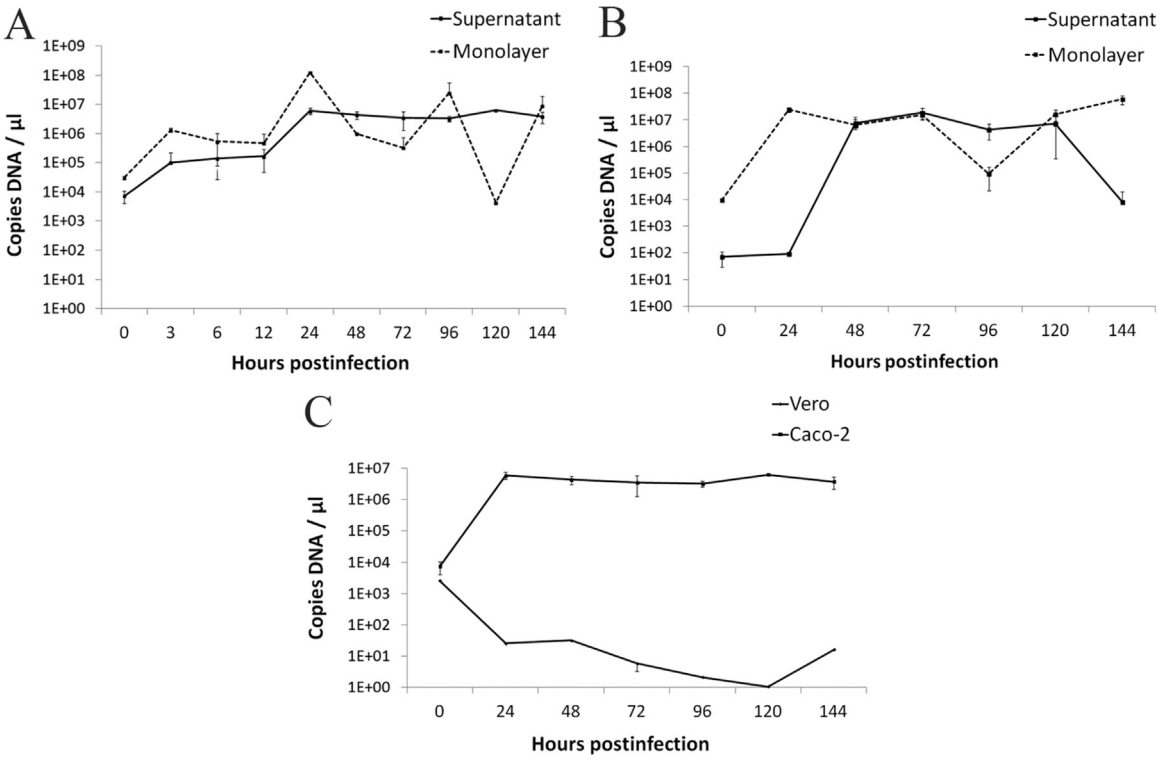

Fig. 3. HBoV1 DNA concentration (copies of DNA/µl) in supernatant and monolayer in culture EMEM-DEAE-dextran at different hours postinfection (x axis) inoculated with sample 307, (A) Caco-2 at 37 °C, (B) Caco-2 at 33 °C, (C) supernatant Vero and Caco-2 culture at 37 °C.

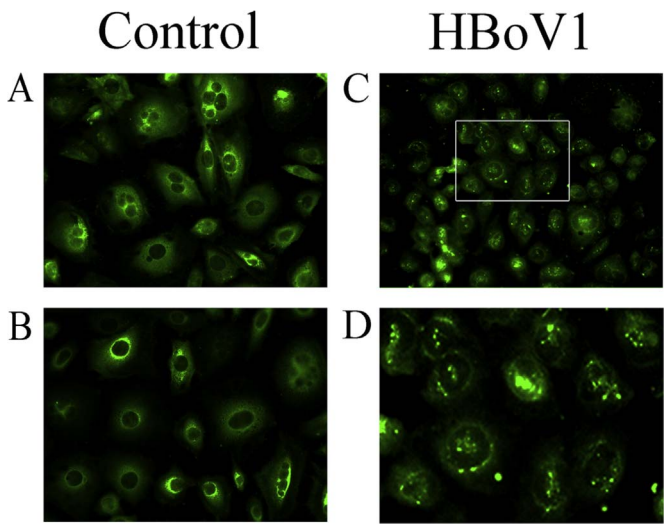

Fig. 5. FITC-immunofluorescence assay on Caco-2 cultures infected with HBoV1 in the presence of EMEM-DEAE-dextran at 24 hpi (C and D). A and B: Control cultures (inoculated with sterile medium and a negative clinical specimen, respectively). A, B and C: 60X; D: detail of photo C.

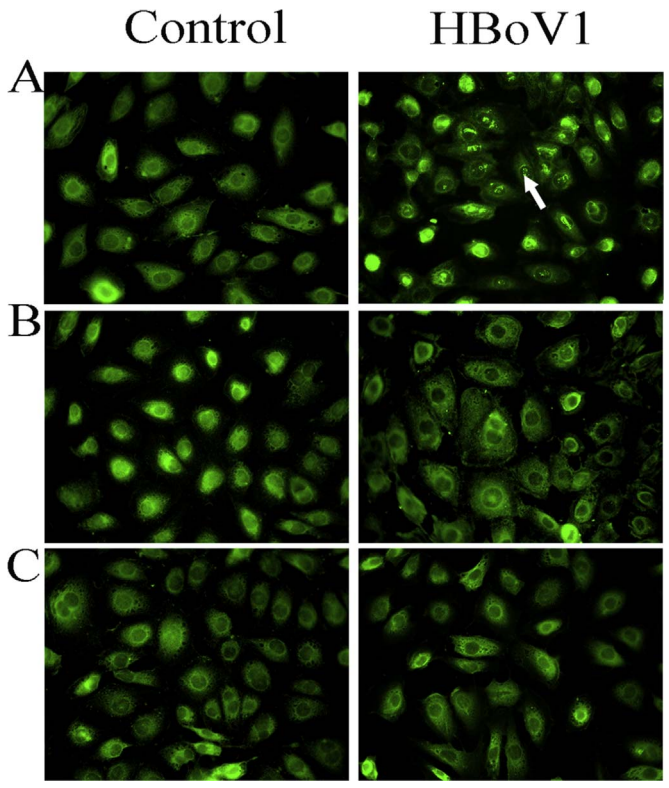

Fig. 6. Caco-2 cell infected with HBoV1 in the presence of MEME-DEAE-dextran stained by FITC-immunofluorescence assay, 24 hpi. A: Assay without antibody capture, B: Antibody capture with positive supernatant, C: Antibody capture with positive monolayer. 60X.

supernatant, we obtained a segmented sequence from nucleotide 1–1937 (GenBank accession number KY629422) and from nucleotide 2407–4277 (KY629423), missing two fragments from nucleotide 1938–2406 and 3' extreme from nucleotide 4278, which we were not able to amplify with the available primers. These gaps corresponded to fragments in the genes coding for NS1 and VP1/VP2 proteins, respectively. The virus in the monolayer was sequenced completely (KY629421). When the obtained sequences from the monolayer and

Table 2
Mutations observed in the DNA sequence of HBoV1 obtained from Caco-2 culture supernatant and monolayer at 6 dpi.

	DNA mutation	Location	Gen	Protein mutation
Supernatant	C-T	1388	NS1	T-I
		1465	NS1	
		1470	NS1	F-L
		1477	NS1	
		1512	NS1	
	A-G	1793	NS1	Y-C
		1811	NS1	N-R[a]
		1849	NS1	R-G
		1878	NS1	
		1903	NS1	T-A
	G-A	1795	NS1	A-T
	A-T	1735	NS1	R-[b]
		1784	NS1	H-L
		1843	NS1	K-[b]
	T-A	1892	NS1	F-Y
	G-T	1786	NS1	D-Y
		1914	NS1	
	T-G	1867	NS1	F-V
		1911	NS1	E-D
	A-C	1810	NS1	N-R[a]
		1874	NS1	K-T
	C-A	1437	NS1	
		1445	NS1	P-H
		1491	NS1	
	C-G	1928	NS1	L-R
Monolayer	C-T	1927	NS1	
		2397	-	
		2445	NP1	
	A-G	2050	NS1	T-A
	A-T	2432	NP1	D-V
	T-A	2250	-	
	C-A	2023	NS1	L-I
	C-G	2070	NS1	Y-[b]

[a] Mutation in the same codon.
[b] Stop codon.

the supernatant were compared to the HBoV1 reference strain isolated from clinical sample 307 (KJ634207) we detected 33 mutations in total, all located in the nonstructural genes and mainly in the NS1 sequence, as shown in Table 2. These nucleotide changes were associated with mutations in 17 amino acids in the virus from the supernatant, two of them were transversion mutations (A-T) which led to the occurrence of stop codons. In the monolayer we detected four aminoacidic mutations. One of them, at the amino acid position 606 (NS1 nt 1816–1818) is a C-G transversion which brings a change from the amino acid Tyrosine to a stop codon, leading to a truncated protein missing 34 amino acids at the C-terminal extreme (Fig. 7).

4. Discussion

In this study, we present results of infection of Caco-2 cells with HBoV1 from respiratory secretions (either, the infective viral particle or free HBoV1 DNA present in the clinical specimens). We describe HBoV1 infection of Caco-2 cell line utilizing DEAE-dextran, a compound that has been described as facilitator of infection in permissive cells (Carrascosa, 1994; Musich et al., 2015; Pagano and Vaheri, 1965; Scott et al., 2000). We demonstrate infection by detecting HBoV1 genome in the attached cells and in the supernatant medium of the cultures 1–6 dpi), a raise in the concentration of viral DNA, and a unique pattern of immunofluorescence using pooled policlonal antibodies, which evidences the proteins of the virus in the replication sites (1 and 4 dpi). In addition, we corroborated the virus DNA replicated by sequencing the viral genome detected in the supernatant and in the monolayer. In spite of HBoV1 replication in Caco-2 cells after inoculation of respiratory material, the viral progeny is not capable of subsequent infection cycles. This might be an outcome of different

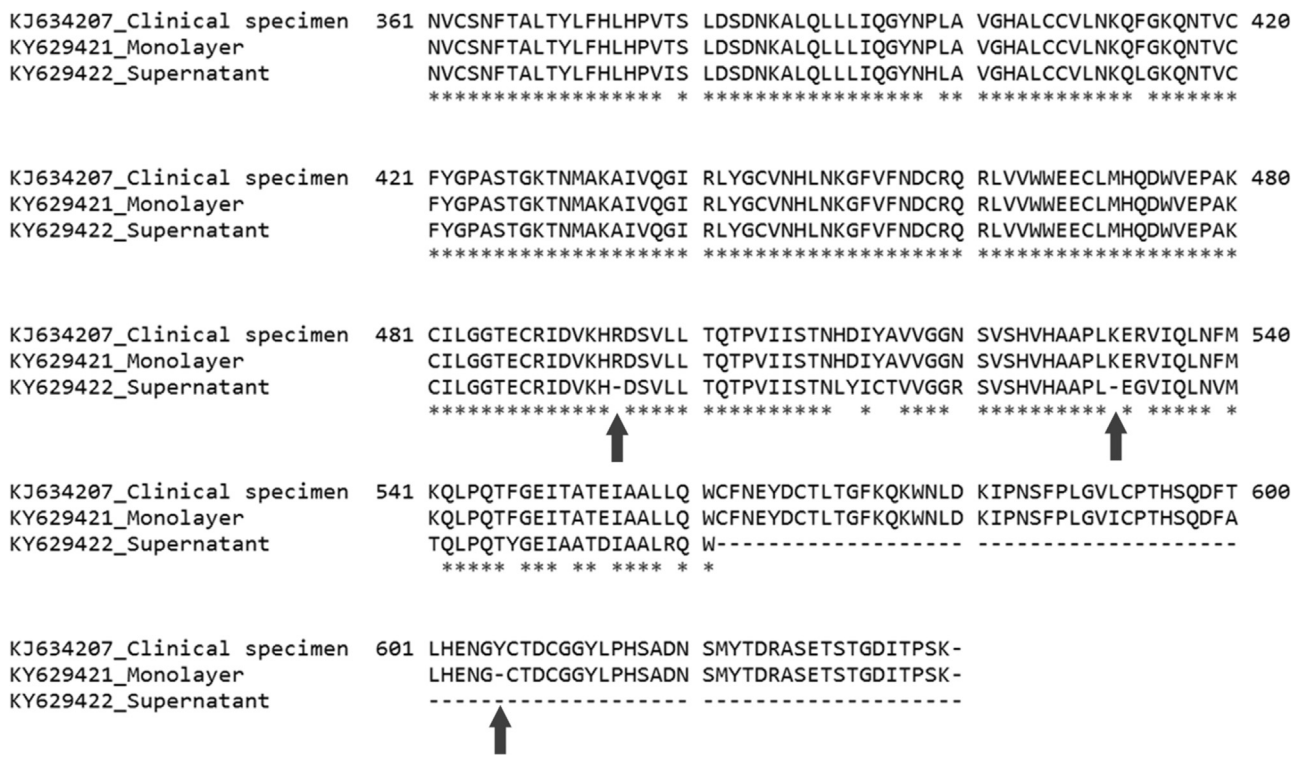

Fig. 7. Comparison of NS1 protein sequence of KJ634207 to the sequences obtained from Caco-2 cells (monolayer and supernatant), from 481 to 639 aa. The arrows indicate stop codon mutations in the aminoacid position.

and possibly overlapping mechanisms of virus-cell interactions, including mutations in the progeny genome that have a profound effect in the viral protein functions, namely the virus entry and genome replication. Overall, these results can provide insights into the observations that HBoV1 can be detected in human tissues other than the respiratory epithelium (Gunel et al., 2015; Norja et al., 2012; Schildgen et al., 2013). In Caco-2 cell cultures infected with HBoV1 and supplemented with DEAE-dextran (1 μg/ml) at 33 °C and 37 °C, the presence of HBoV1 was observed in the supernatants and the cells attached to the substrate from 1 to 6 dpi, in contrast to cultures maintained with standard EMEM (Table 1 and Fig. 3A and B). As a confirmation that the virus enters in these cells, the same procedures applied to Vero cultures, used as a reference since it has been documented previously that HBoV1 does not replicate in this cells line (Huang et al., 2012), do not result in detection of the viral DNA (Table 1 and Fig. 3C). Immunofluorescence assays confirmed HBoV1 infection in Caco-2 culture supplemented with DEAE-dextran (Fig. 5). Scattered foci of a spotted pattern located in the periphery of the nucleus and nuclear membrane was consistently observed in infected monolayers at 24 and 96 hpi. This picture was not detected in the uninfected cultures and furthermore, the primary antibody capture assays prevented it (Fig. 6). Since the capture assays were performed with supernatant medium and lysates from attached cells of infected cultures, these assays not only confirm the HBoV1 immunofluorescence pattern but also the presence of neutralizing viral particles and/or proteins in the cultures. Regarding the fluorescence pattern, our findings agree with those of Schildgen and coworkers (Schildgen et al., 2013), who described a FISH analysis on tumor tissue samples and on transfected HepG2 cells with probes targeting the regions near the left and right end hairpins. From their assays, the authors depict a perinuclear specific fluorescence in both types of samples; in addition, in tumor tissues the staining pattern was heterogeneous: some samples had a single hairpin signal per infected cell, while multiple signals were detected in other samples, suggestive of chronic or latent HBoV1 infection congruent with a model of replication in a focal manner.

Quantitation of virus in the supernatants and attached Caco-2 cells of cultures infected with low- or high-virus titer inoculum, maintained at 37 °C with DEAE-dextran, shows a progressive increase of HBoV1 DNA copies/μl in the first 48 h. After that, the viral genome remained high and relatively constant for the period that the experiment lasted (6 days, Fig. 3A). These results evidence a viral replication cycle of rapid development, even when the cells are differentiated (enterocyte type, Fig. 4) and match the data obtained by other authors using HAE-ALI cell cultures, which show an increase in the viral titer during the first 72 hpi when inoculated at a high MOI (Deng et al., 2014). In contrast, at 33 °C (a temperature close to that in the upper airway tract) the virus replication apparently is delayed and HBoV1 DNA is detected in the supernatant later, compared to 37 °C (Fig. 3B). While this might only represent an effect of the lower metabolic rate of Caco-2 cells at 33 °C, it is important to note that HBoV1 still replicates in this condition. Thus, it is worth investigating if these findings correlate with the capacity of the virus to produce both upper and lower respiratory tract infections, as well as comparing the genome sequences of viruses isolated from upper and lower tract. It has been shown that a single amino acid change in PB2 protein of H5N1 Influenza virus can confer the advantage for efficient growth in the upper and lower respiratory tract (Hatta et al., 2007). Therefore, it can be hypothesized that the ability to replicate in different conditions and tissues might be related to the pathogenesis of HBoV1.

HBoV1 genome load increase right after the first 24 h post-inoculation, as well as the presence of viral proteins (presumably structural and non-structural, assuming antibodies against both types of viral proteins in the polyclonal pooled-sera of children with confirmed infection) both endorse virus entrance and replication in Caco-2 cells. However, the results of blind passages of supernatants and monolayers indicate that the infection in Caco-2 cells is limited. In addition to this, the assays with differentiated Caco-2 cells indicate that the virus is not release to the supernatant and the viral genome is detected only in the monolayer after 28 dpi and at very low concentration. Since the viral genome and proteins can be detected in the supernatant medium and cells of the initial cultures of these series but both fail to infect a new culture, it can also be inferred that the viral

progeny contains no infective particles. Different and non-excluding mechanisms could explain those outcomes.

On the one hand, the action of the cell-autonomous innate immune system response could be limiting and controlling the infection. Type I interferons (IFN) are induced by simultaneous multiple ways that allow the cells to detect virus infection (Randall and Goodbourn, 2008). Caco-2 cells have a functional IFN system (Cuadras et al., 2002; Guix et al., 2015). HBoV1 innate immune response: it has been shown that the VP2 protein induces the expression of IFN-β by physically interacting with the negative regulator RNF125 (Luo et al., 2013). Conversely, another report shows that the NP1 protein has the ability to inhibit activation of IFN-β by preventing the binding of transcription factor IRF-3 with the corresponding promoter (Zhang et al., 2012). Although the puzzle is not complete, these data provide an example of how HBoV1 can activate and influence the balance in IFN production. IFN action could even justify the pattern of scattered foci of infected cells that we observed in immunofluorescence tests (Fig. 5). In a scenario that is common to many viruses (Randall and Goodbourn, 2008), we could speculate that NP1 and VP2 proteins of HBoV1 alternately affect IFN synthesis in the target tissue for the benefit of the virus: first to delay apoptosis (which reportedly prevents the generation of virus progeny) and later to accelerate the release and dissemination of new virus particles to susceptible cells. These mechanisms suggest a preponderant role of IFN in the first cellular response to HBoV1 infection, which can be explored in Caco-2 cells.

On the other hand, the generation of defective interfering viral particles (DIVP) could also determine the fall of infective virus titer. DIVP were identified over 40 years ago (Huang and Baltimore, 1970; Lazzarini et al., 1981). They can result from errors in the polymerase enzyme activity when replicating nucleic acids, which can generate changes or deletions in genes important for virus assembly or for function of structural proteins resulting in problems in the interaction with the target cell. We attempted sequencing and comparing the entire genomes of the input virus and the progeny (in the monolayers and in the supernatants) at 6 dpi. It was not possible to sequence two segments (out of 8 overlapping fragments) corresponding to NS1 and VP1/VP2 proteins from the virus detected in the supernatants, probably due to a number of mutations in the sites of primer binding. However, we were able to obtain a complete genome sequence from the virus in the monolayers. Comparing the sequences obtained from the culture to the virus in the clinical specimen, we observed other 33 mutations located mostly in NS1 protein. We specifically detected a mutation that reverts to a stop codon, which results in a truncated NS1 protein (Table 2 and Fig. 7). This important number of changes at the end of the coding sequence bearing the helicase domain could explain, at least in part, the absence of infective viral progeny particles in our Caco-2 cultures. HBoV1 NS1 contains an N-terminal DNA binding/endonuclease domain, a central helicase domain, and a C-terminal zinc-finger domain (Chen et al., 2010; Dijkman et al., 2009; Shen et al., 2015), functions that account for non-structural protein NS1 key roles in the viral life cycle of parvoviruses, such as genome transcription, replication, and packaging (Cotmore and Tattersall, 2013). In addition, some authors observed that HBoV1 genome exists as head-to-tail monomer in infected tissues, which either reflects the likely evolution of alternative replication mechanism in primate bocaviruses or a mechanism of viral persistence (Kapoor et al., 2011; Lusebrink et al., 2011). It would be interesting to determine the presence of head-to-tail intermediates in the attached Caco-2 cells (of both, standard and differentiated cultures), as well as performing assays with clinical specimens pre-treated with DNase in order to ensure infection with viral particles and not free viral DNA. Together with the novel sequence information reported here, it would increase our understanding of HBoV1 infection and contribute to the future development of HBoV1 cell culture models.

In conclusion, we show that HBoV1 directly isolated from respiratory clinical samples can infect standard and differentiated cultures of Caco-2 cells. These cultures may be useful for future research on HBoV1 receptor and virus-cell interactions, including insights into HBoV1 infection, replication, innate response, persistence and potential pathogenic role in tumors.

Conflict of interest

All authors declare that they have no conflict of interest.

Acknowledgments

This study was funded with grants from Fundación Alberto J. Roemmers, Secretaría de Ciencia y Tecnología (Universidad Nacional de Córdoba) (05/H363), and FONCyT (Agencia Nacional de Promoción Científica y Tecnológica, Argentina) (PICT-2016-4445). L. M. G. is a recipient of a post-doctoral fellowship from Consejo Nacional de Investigaciones Científicas y Técnicas (CONICET) (Resol. D Nº 4885/2015).

References

Abdel-Moneim, A.S., El-Fol, H.A., Kamel, M.M., Soliman, A.S., Mahdi, E.A., El-Gammal, A.S., Mahran, T.Z., 2016. Screening of human bocavirus in surgically excised cancer specimens. Arch. Virol..

Allander, T., Jartti, T., Gupta, S., Niesters, H.G., Lehtinen, P., Osterback, R., Vuorinen, T., Waris, M., Bjerkner, A., Tiveljung-Lindell, A., van den Hoogen, B.G., Hyypia, T., Ruuskanen, O., 2007. Human bocavirus and acute wheezing in children. Clin. Infect. Dis. 44, 904–910.

Bicer, S., Giray, T., Col, D., Erdag, G.C., Vitrinel, A., Gurol, Y., Celik, G., Kaspar, C., Kucuk, O., 2013. Virological and clinical characterizations of respiratory infections in hospitalized children. Ital. J. Pediatr. 39, 22.

Buhrke, T., Lengler, I., Lampen, A., 2011. Analysis of proteomic changes induced upon cellular differentiation of the human intestinal cell line Caco-2. Dev. Growth Differ. 53, 411–426.

Cardozo Tomas, A., Ghietto, L.M., Insfran, C., Wasinger, N., Marchesi, A., Adamo, M.P., 2015. First report of complete genome sequence and phylogenetic analysis of human Bocavirus 1 isolated in Argentina. Rev. Fac. Cienc. Med. 72, 161–169.

Carrascosa, A.L., 1994. Enhancement of baculovirus plaque assay in insect cell monolayers by DEAE-dextran. BioTechniques 16, 1078–1081, (1083-1075).

Chen, A.Y., Cheng, F., Lou, S., Luo, Y., Liu, Z., Delwart, E., Pintel, D., Qiu, J., 2010. Characterization of the gene expression profile of human bocavirus. Virology 403, 145–154.

Christensen, A., Nordbo, S.A., Krokstad, S., Rognlien, A.G., Dollner, H., 2010. Human bocavirus in children: mono-detection, high viral load and viraemia are associated with respiratory tract infection. J. Clin. Virol. 49, 158–162.

Cotmore, S.F., Tattersall, P., 2013. Parvovirus diversity and DNA damage responses. Cold Spring Harb. Perspect. Biol., 5.

Cuadras, M.A., Feigelstock, D.A., An, S., Greenberg, H.B., 2002. Gene expression pattern in Caco-2 cells following rotavirus infection. J. Virol. 76, 4467–4482.

Deng, X., Yan, Z., Luo, Y., Xu, J., Cheng, F., Li, Y., Engelhardt, J.F., Qiu, J., 2013. In vitro modeling of human bocavirus 1 infection of polarized primary human airway epithelia. J. Virol. 87, 4097–4102.

Deng, X., Li, Y., Qiu, J., 2014. Human bocavirus 1 infects commercially available primary human airway epithelium cultures productively. J. Virol. Methods 195, 112–119.

Dijkman, R., Koekkoek, S.M., Molenkamp, R., Schildgen, O., van der Hoek, L., 2009. Human bocavirus can be cultured in differentiated human airway epithelial cells. J. Virol. 83, 7739–7748.

Gangl, K., Waltl, E.E., Vetr, H., Cabauatan, C.R., Niespodziana, K., Valenta, R., Niederberger, V., 2015. Infection with rhinovirus facilitates allergen penetration across a respiratory epithelial cell layer. Int. Arch. Allergy Immunol. 166, 291–296.

Garcia-Garcia, M.L., Calvo, C., Pozo, F., Perez-Brena, P., Quevedo, S., Bracamonte, T., Casas, I., 2008. Human bocavirus detection in nasopharyngeal aspirates of children without clinical symptoms of respiratory infection. Pediatr. Infect. Dis. J. 27, 358–360.

Ghietto, L.M., Camara, A., Camara, J., Adamo, M.P., 2012a. High frequency of human bocavirus 1 DNA in infants and adults with lower acute respiratory infection. J. Med. Microbiol. 61, 548–551.

Ghietto, L.M., Camara, A., Zhou, Y., Pedranti, M., Ferreyra, S., Frey, T., Camara, J., Adamo, M.P., 2012b. High prevalence of human bocavirus 1 in infants with lower acute respiratory tract disease in Argentina, 2007–2009. Braz. J. Infect. Dis. 16, 38–44.

Ghietto, L.M., Majul, D., Ferreyra Soaje, P., Baumeister, E., Avaro, M., Insfran, C., Mosca, L., Camara, A., Moreno, L.B., Adamo, M.P., 2015. Comorbidity and high viral load linked to clinical presentation of respiratory human bocavirus infection. Arch. Virol. 160, 117–127.

Guix, S., Perez-Bosque, A., Miro, L., Moreto, M., Bosch, A., Pinto, R.M., 2015. Type I interferon response is delayed in human astrovirus infections. PLoS One 10, e0123087.

Gunel, C., Kirdar, S., Omurlu, I.K., Agdas, F., 2015. Detection of the Epstein-Barr virus,

human bocavirus and novel KI and KU polyomaviruses in adenotonsillar tissues. Int. J. Pediatr. Otorhinolaryngol. 79, 423–427.
Hatta, M., Hatta, Y., Kim, J.H., Watanabe, S., Shinya, K., Nguyen, T., Lien, P.S., Le, Q.M., Kawaoka, Y., 2007. Growth of H5N1 influenza A viruses in the upper respiratory tracts of mice. PLoS Pathog. 3, 1374–1379.
Huang, A.S., Baltimore, D., 1970. Defective viral particles and viral disease processes. Nature 226, 325–327.
Huang, Q., Deng, X., Yan, Z., Cheng, F., Luo, Y., Shen, W., Lei-Butters, D.C., Chen, A.Y., Li, Y., Tang, L., Soderlund-Venermo, M., Engelhardt, J.F., Qiu, J., 2012. Establishment of a reverse genetics system for studying human bocavirus in human airway epithelia. PLoS Pathog. 8, e1002899.
Kapoor, A., Hornig, M., Asokan, A., Williams, B., Henriquez, J.A., Lipkin, W.I., 2011. Bocavirus episome in infected human tissue contains non-identical termini. PLoS One 6, e21362.
Khalfaoui, S., Eichhorn, V., Karagiannidis, C., Bayh, I., Brockmann, M., Pieper, M., Windisch, W., Schildgen, O., Schildgen, V., 2016. Lung infection by human bocavirus induces the release of profibrotic mediator cytokines in vivo and in vitro. PLoS One 11, e0147010.
Lazzarini, R.A., Keene, J.D., Schubert, M., 1981. The origins of defective interfering particles of the negative-strand RNA viruses. Cell 26, 145–154.
Lnenickova, K., Prochazkova, E., Skalova, L., Matouskova, P., Bartikova, H., Soucek, P., Szotakova, B., 2016. Catechins variously affect activities of conjugation enzymes in proliferating and differentiated caco-2 cells. Molecules, 21.
Luo, H., Zhang, Z., Zheng, Z., Ke, X., Zhang, X., Li, Q., Liu, Y., Bai, B., Mao, P., Hu, Q., Wang, H., 2013. Human bocavirus VP2 upregulates IFN-beta pathway by inhibiting ring finger protein 125-mediated ubiquitination of retinoic acid-inducible gene-I. J. Immunol. 191, 660–669.
Lusebrink, J., Schildgen, V., Tillmann, R.L., Wittleben, F., Bohmer, A., Muller, A., Schildgen, O., 2011. Detection of head-to-tail DNA sequences of human bocavirus in clinical samples. PLoS One 6, e19457.
Martin, E.T., Taylor, J., Kuypers, J., Magaret, A., Wald, A., Zerr, D., Englund, J.A., 2009. Detection of bocavirus in saliva of children with and without respiratory illness. J. Clin. Microbiol. 47, 4131–4132.
Meriluoto, M., Hedman, L., Tanner, L., Simell, V., Makinen, M., Simell, S., Mykkanen, J., Korpelainen, J., Ruuskanen, O., Ilonen, J., Knip, M., Simell, O., Hedman, K., Soderlund-Venermo, M., 2012. Association of human bocavirus 1 infection with respiratory disease in childhood follow-up study, Finland. Emerg. Infect. Dis. 18, 264–271.
Musich, T., O'Connell, O., Gonzalez-Perez, M.P., Derdeyn, C.A., Peters, P.J., Clapham, P.R., 2015. HIV-1 non-macrophage-tropic R5 envelope glycoproteins are not more tropic for entry into primary CD4+ T-cells than envelopes highly adapted for macrophages. Retrovirology 12, 25.
Nascimento-Carvalho, C.M., Cardoso, M.R., Meriluoto, M., Kemppainen, K., Kantola, K., Ruuskanen, O., Hedman, K., Soderlund-Venermo, M., 2012. Human bocavirus infection diagnosed serologically among children admitted to hospital with community-acquired pneumonia in a tropical region. J. Med. Virol. 84, 253–258.
Norja, P., Hedman, L., Kantola, K., Kemppainen, K., Suvilehto, J., Pitkaranta, A., Aaltonen, L.M., Seppanen, M., Hedman, K., Soderlund-Venermo, M., 2012. Occurrence of human bocaviruses and parvovirus 4 in solid tissues. J. Med. Virol. 84, 1267–1273.
Pagano, J.S., Vaheri, A., 1965. Enhancement of infectivity of poliovirus RNA with diethylaminoethyl-dextran (DEAE-D). Arch. fur die Gesamt. Virusforsch. 17, 456–464.
Papadopoulos, N.G., Sanderson, G., Hunter, J., Johnston, S.L., 1999. Rhinoviruses replicate effectively at lower airway temperatures. J. Med. Virol. 58, 100–104.
Qiu, J., Soderlund-Venermo, M., Young, N.S., 2017. Human parvoviruses. Clin. Microbiol. Rev. 30, 43–113.
Randall, R.E., Goodbourn, S., 2008. Interferons and viruses: an interplay between induction, signalling, antiviral responses and virus countermeasures. J. Gen. Virol. 89, 1–47.
Schildgen, V., Malecki, M., Tillmann, R.L., Brockmann, M., Schildgen, O., 2013. The human bocavirus is associated with some lung and colorectal cancers and persists in solid tumors. PLoS One 8, e68020.
Scott, G.M., Ratnamohan, V.M., Rawlinson, W.D., 2000. Improving permissive infection of human cytomegalovirus in cell culture. Arch. Virol. 145, 2431–2438.
Shen, W., Deng, X., Zou, W., Cheng, F., Engelhardt, J.F., Yan, Z., Qiu, J., 2015. Identification and functional analysis of novel nonstructural proteins of human bocavirus 1. J. Virol. 89, 10097–10109.
Vaheri, A., Pagano, J.S., 1965. Infectious poliovirus RNA: a sensitive method of assay. Virology 27, 434–436.
Wang, K., Wang, W., Yan, H., Ren, P., Zhang, J., Shen, J., Deubel, V., 2010. Correlation between bocavirus infection and humoral response, and co-infection with other respiratory viruses in children with acute respiratory infection. J. Clin. Virol. 47, 148–155.
Zhang, Z., Zheng, Z., Luo, H., Meng, J., Li, H., Li, Q., Zhang, X., Ke, X., Bai, B., Mao, P., Hu, Q., Wang, H., 2012. Human bocavirus NP1 inhibits IFN-beta production by blocking association of IFN regulatory factor 3 with IFNB promoter. J. Immunol. 189, 1144–1153.